International Journal of Aerospace and Lightweight Structures
Vol. 1, No. 1 (2011) 133–142
© Research Publishing Services
DOI: 10.3850/S2010428611000055

SUPERSONIC UNSTEADY FLOW AROUND A CAPSULE-SHAPED ABORT SYSTEM WITH ANGLE OF ATTACK

YUNPENG WANG* and YOSHIAKI NAKAMURA†
Aerospace Engineering, Nagoya University
Nagoya, 464-8603, Japan

Accepted 6 September 2011

Supersonic flow over a capsule-shaped abort system with angle of attack (AoA) of α, which is boosted by supersonic aerodynamic interference, is investigated numerically through the 3D simulation. The objective of this study is to examine the effects of AoA on aerodynamic stability. In the previous study, the flowfield around this system at $\alpha = 0°$ is unsteady and has a strong periodic flow oscillation in the case without the clearance between the capsule and rocket. In the present study, this system has the angle of attack and a disk is installed to enhance the abort separation. The self-sustaining flow oscillation in the case with AoA is described and is visualized using the phase-averaged analysis of simulated results. With increasing AoA, the oscillating flow is divided into two parts, which correspond to the lower and upper surfaces of the cone. These two flows have a phase difference which becomes larger with increasing AoA. The present findings show it is about 0.28π and 0.4π, respectively. At the same time, the lower flow oscillation is out of step with the upper one, and an inharmonic flow oscillation occurs because of strong aerodynamic interaction in the lower flow. This unstable flow will lead to a risky abort separation and this phenomenon is analyzed in detail in this paper.

Keywords: Abort system; Flow oscillation; AoA; Interference; Unsteady flow.

1. Introduction

The space shuttle orbiters has been retired in 2011 after they have played an active role in the USA space program for more than a quarter century. They will be replaced by a new human-rated rocket and crewed capsule, i.e., a new space transportation system (STS) using a capsule/rocket configuration such as Apollo and Soyuz [Pandya *et al.*, 2006], [Pulsonetti and Thompson, 2004]. In NASA's Constellation project, the Orion spacecraft consists of a crew module (CM), Service Module (SM), and Launch Abort System (LAS), which are similar in design to the Apollo space capsules [Williams-Hayes, 2007].

In the event of a catastrophic failure on the launch pad or during the early ascent phase of the space transportation system, LAS will initiate an abort that will pull

*PhD student, wang@fluid.nuae.nagoya-u.ac.jp
†Professor, nakamura@nuae.nagoya-u.ac.jp

the capsule to a safe distance away from the launch pad or the rocket. Therefore, the abort scenario was a topic of study during the Apollo mission because of its importance; it is the only method for saving the astronauts in case of a disaster [Davidson, 2007], [Chan *et al.*, 2008]. Here in this study, a capsule-shaped abort system using aerodynamic interference is proposed, in which a rocket with a disk is considered. Ozawa, H. *et al.*, [2009] conducted experiment on this escape system using a static model and analyzed the phenomenon of flow oscillation for the case without AoA. The very strong aerodynamic interaction can be used for the abort system. Wang, Y. *et al.*, [2011] simulated the abort separation of this system using a series of static and dynamic models, and analyzed the effect of Mach number on self-sustained flow oscillations in the case without separation distance.

However, these results are based on the case of zero attack angle: $\alpha = 0°$. In this study, the effect of AoA, namely, change in the flowfield and aerodynamic interaction for various angles of attack, is examined using a series of static, viscous simulations for the case without separation distance and using the phase-averaged analysis for these results. The phenomena of self-sustaining flow oscillation for the cases at different AoAs are compared at the same phase. The result of numerical pressure at $M = 3.0$ is compared with wind tunnel data in the case of $\alpha = 5°$. Numerical results of surface-flow are presented to show two separated flows on the surface of capsule and a phase difference.

2. Numerical Methods

2.1. *Computational conditions*

Supersonic flow around a capsule-shaped space transportation system at different AoA is studied by CFD simulation, and the experiment presented in this paper is carried out at the Institute of Space and Astronautical Science of the Japan Aerospace Exploration Agency (ISAS/JAXA). In the present study, the rocket uses a disk to boost the thrust force for the abort separation between the capsule and rocket. The disk has a diameter of $1.48D$ and a thickness of 10 mm, where D is the maximum diameter of the capsule. The angle of attack is set to $\alpha = 0\,°$, $1\,°$, $3\,°$, $5\,°$, and $8\,°$. Figure 1 shows the model employed in this study along with the definition of angle of attack. The location of data collection points used in the analysis mentioned later are also defined in this figure.

Mach number is set to 3.0 throughout this paper. The AoA is changed through setting the direction of uniform flow. Table 1 shows the freestream conditions used in the current study.

2.2. *Governing equations, algorithm and grid*

Computations were carried out using a parallel, sructured, single-block, inhouse code, where the three-dimensional (3D) compressible Navier-Stokes equations are discretized by the cell vertex finite volume method. Jameson-Baker's four-stage Runge-Kutta method was employed for time integration [Jameson and Baker, 1983],

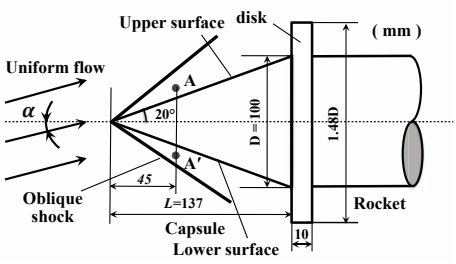

Fig. 1. Schematic of definition of AoA and the location of data collection points.

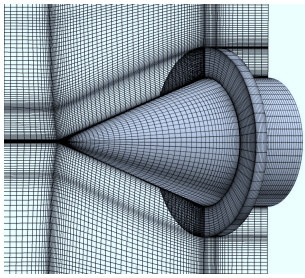

Fig. 2. 3D view of computational grid.

Table 1. Freestream Conditions.

M_∞	Re	P_0 (kpa)	P_∞ (kpa)	T_0 (K)
3.0	2.3×10^6	2.2×10^5	6.0×10^3	292

and the Simple High-resolution Upwind Scheme (SHUS) [Shima and Jounouchi, 1996] to calculate inviscid numerical fluxes at cell interfaces, which is a family of advection upstream splitting method (AUSM) type schemes. In addition, the MUSCL scheme with the van Albada flux limiter is adopted for the third-order accurate numerical solutions. Viscous fluxes are calculated by the second-order central difference. The CFL number is fixed and equals 0.5. As the accuracy of results obtained by the present in-house code has already been confirmed from the previous study [Ozawa *et al.*, 2009], [Wang *et al.*, 2011], it is applied to predict unsteady flow fields in this study. Additionally, the calculations were carried out by an eight-processor Linux cluster, and the MPI (Message Passing Interface) was used for parallelization.

No turbulence model is employed here to show the case for laminar flow. Ozawa [2009] and Wang [2011] have already performed the numerical simulation in the case without the clearance at $\alpha = 0\,^\circ$ using a laminar case, where those results obtained by calculations are in agreement with experimental data. Therefore, the same conditions are employed in this paper, include a similar mesh.

The total number of 3D grid points are 401×250×60 in all the cases, and the minimum grid size is 0.01 mm. The 3D view of the computational domain is shown in Fig. 2, where grid lines are drawn every five lines in the axial direction and every three lines in the radial direction, respectively.

3. Results and Discussion

3.1. *Self-sustaining flow oscillation at different AoAs*

3.1.1. *Phase averaged data*

The method of phase averaging is employed to analyze the self-sustained flow oscillation and to visualize the feedback loop cycle. This technique, as discussed

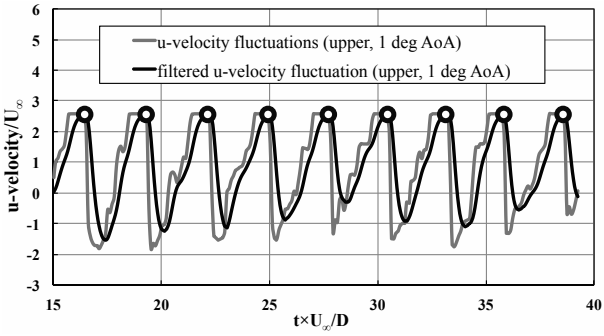

Fig. 3. Determination of the length of period in the case of $\alpha = 1°$.

by Hussain and Reynolds [1970], is based on the triple decomposition of a scalar $\alpha(\alpha, t)$ in an ensemble averaged value $\bar{\alpha}(\boldsymbol{X})$, a cyclic component $\tilde{\alpha}(t)$ and a fluctuating component $\alpha'(t)$. The phase averaged component is then defined as $\langle\alpha\rangle(\boldsymbol{X}, t) = \bar{\alpha}(\boldsymbol{X}) + \tilde{\alpha}(\boldsymbol{X}, t)$. A variant of this procedure introduced by Cantwell and Coles [1983] is used to calculate $\langle\alpha\rangle$ in this study. Before defining the phase, computation is first carried out in order to determine the peaks of the reference filtered quasi-periodic u-velocity (velocity component in the axial direction) signal at the point A in Fig. 1 using the low-pass filter method. This point is located inside the Mach cone; specifically it is 10 mm above the surface of cone and 45 mm downstream from the vertex of cone along the surface.

Figure 3 shows the time-series signals of original u-velocity fluctuations and low-pass filtered ones in the case of $\alpha = 1°$. The highest values, denoted by black circles, of the low-pass filtered signals are defined as the trigger points for phase averaging. In this study, the number of phase angle is set to 26 and the number of averaging to 8 periods. For other cases, i.e., $\alpha = 0°$, $3°$, $5°$, and $8°$, the same definition and procedure are employed to obtain phase averaged numerical results.

3.1.2. *Unsteady flow with self-sustained oscillation*

Detailed analysis of the pulsation shock during one cycle has been made by Ozawa, H. *et al.*, [2009] in the case of $\alpha = 0°$, where the flow oscillations were explained from the unsteady flow fields with aerodynamic interference at four moments: t = T/4, T/2, 3T/4, T during one period T. Wang, Y. *et al.*, [2011] further analyzed the mechanism of oscillating flow, which is focused on the fluid-fluid and fluid-body interactions. In order to avoid unnecessary duplication, only variations of the flow field at an angle of attack are shown and explained in detail in this study.

Figure 4 shows four phases of the feedback loop in terms of flow oscillation using the phase averaged results for the cases of $\alpha = 5°$; this case has typical characteristics for change in AoA in the range between $\alpha = 0°$ and $8°$. In the case

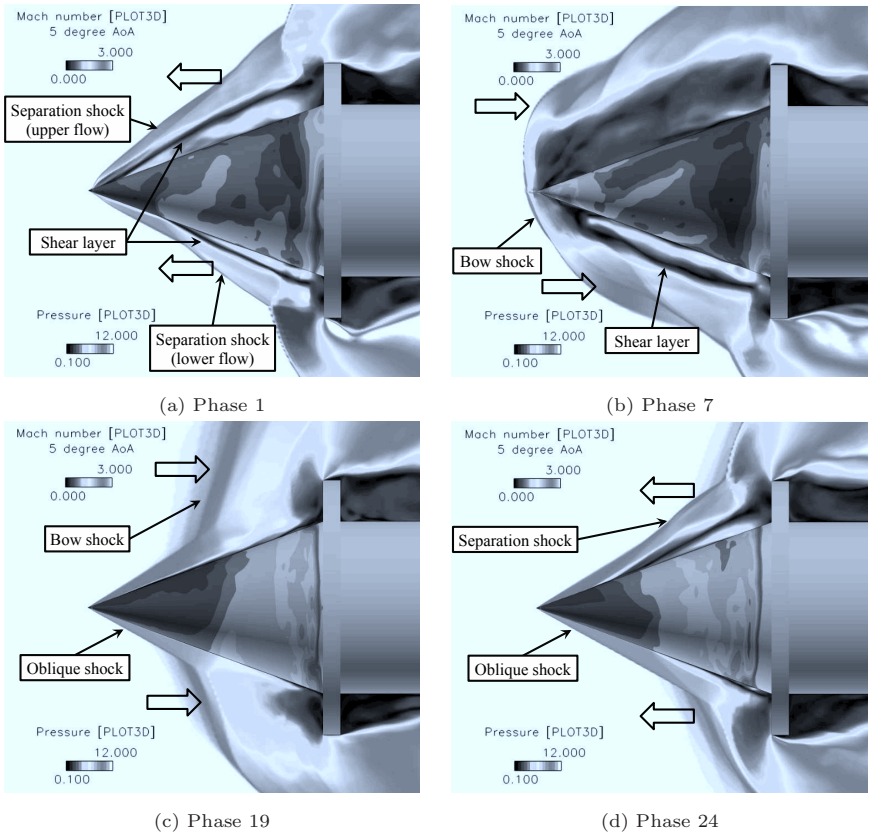

(a) Phase 1 (b) Phase 7

(c) Phase 19 (d) Phase 24

Fig. 4. Visualization of feedback loop using phase averaged data for the case of $\alpha = 5\,^\circ$.

with a small AoA, $\alpha = 1\,^\circ$, the flow field and shock/shock interaction are similar to the case with $\alpha = 0\,^\circ$. However, the flows on the upper and lower surfaces of the cone become different with increasing AoA. The phase 24 result shows that the separated flow on the upper surface is more developed than that on the lower surface [see Fig. 4(d)]. Therefore, its separation shock wave arrives at the cone vertex earlier than the lower one, and generates the bow shock wave [see Figs. 4(a) and (b)]. After that, the bow shock wave gets back and impinges on the separated flow on the lower surface of the cone, which is moving toward the cone vertex.

The flow below the capsule becomes very unstable because of the bow-shock/separation-shock interaction in the lower flowfield. The phase 19 shows the bow shock waves are retreating toward the downstream [see Fig. 4(c)]. Then, the phase 24 will occur again; thus, the feedback loop will be closed. It is found from the numerical results that there is a phase difference between the two separated flows on the upper and lower cone surfaces, which becomes larger with increasing

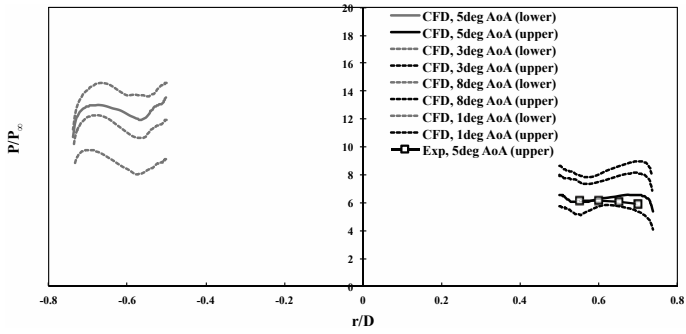

Fig. 5. Time averaged pressure distributions on the surface of disk using phase averaged data.

AoA. In the following section, discussion is made on inharmonic flow oscillation due to this phase difference, leading to bow-shock/separation-shock interaction.

3.2. *Inharmonic flow oscillation*

The non-zero AoA causes the phase difference and the non-uniform pressure distribution on the disk surface. Figure 5 shows the time averaged pressure distributions using the phase averaged data for the cases with $\alpha = 1\,^\circ$, $3\,^\circ$, $5\,^\circ$, and $8\,^\circ$. These results show that the pressure on the lower disk surface is higher than that on the upper one, the difference of which becomes larger with increasing AoA. The numerical result agrees with the experiment data in the case of $\alpha = 5\,^\circ$.

When AoA is rather large, the separated flow is divided into two parts due to the phase difference mentioned above. This phenomenon is shown in Fig. 6 using a series of instantaneous flowfields during one cycle, because the phase averaged data deteriorate the resolution on the visualization of Mach and compression waves. The phase 25 shows that the separated flow is moving toward the cone vertex. In the case of $\alpha = 0\,^\circ$, flow is more stable because there is no phase difference, while in the case of $\alpha = 3\,^\circ$, there are two separated flows on the upper and lower cone surfaces. The phase difference becomes more larger in the case of $\alpha = 8\,^\circ$. In the phase 4, the bow shock wave is retreating. As mentioned above, the bow shock wave, which comes from the upper separation shock, impinges upon the lower separation shock and prevents it from moving forward, where the bow-shock/separation-shock interaction occurs. Thus, the flow becomes more unstable in the case of $\alpha = 8\,^\circ$, especially in the lower flowfield.

The pressure time history at two points: A and A' in Fig. 1 is shown in Fig. 7, where T_{α° is a time period and PD_{α° is the phase difference in the cases with AoAs. The stage I indicates the separation shock wave moves toward the cone vertex, and the stage II shows the bow shock wave is retreating. In the present results, the time averaged phase difference over eight cycles, are $PD_{1^\circ} = 0.04\pi$,

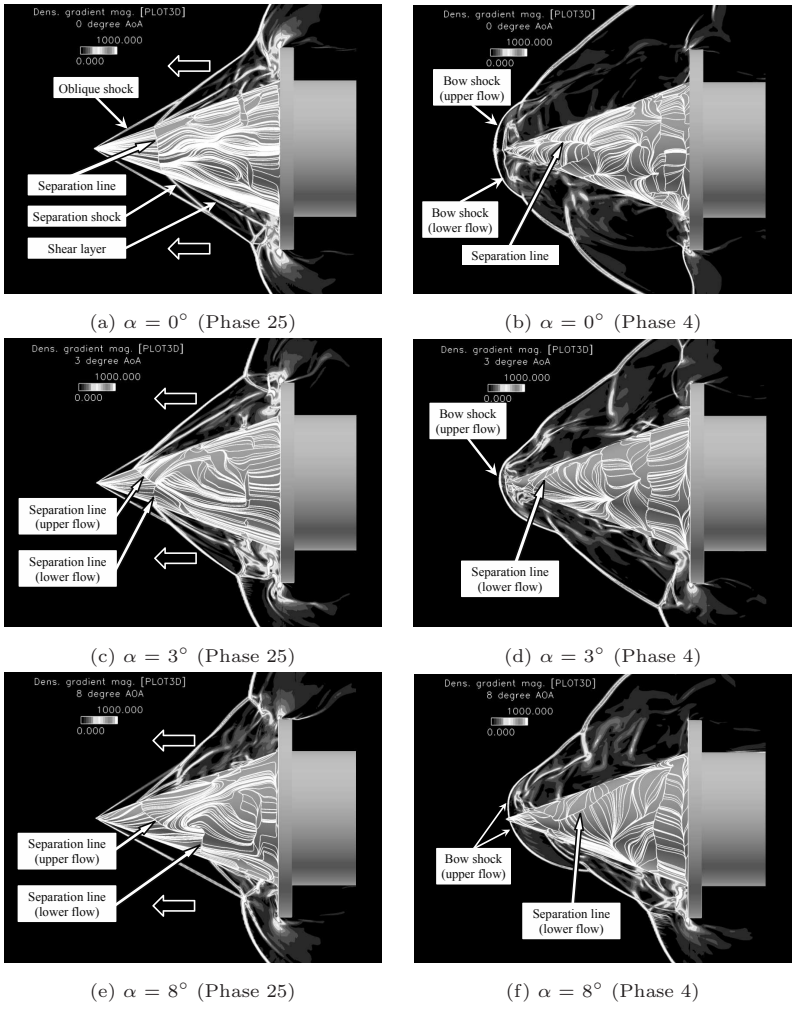

(a) $\alpha = 0^\circ$ (Phase 25) (b) $\alpha = 0^\circ$ (Phase 4)

(c) $\alpha = 3^\circ$ (Phase 25) (d) $\alpha = 3^\circ$ (Phase 4)

(e) $\alpha = 8^\circ$ (Phase 25) (f) $\alpha = 8^\circ$ (Phase 4)

Fig. 6. Density gradient magnitude contours and surface-flow on cone.

$PD_{3^\circ} = 0.12\pi$, $PD_{5^\circ} = 0.28\pi$, and $PD_{8^\circ} = 0.4\pi$ for the cases of $\alpha = 1^\circ$, 3°, 5°, and 8°, respectively.

Furthermore, the time signal of the pressure at point A' shows inharmonic oscillation, especially in the case of $\alpha = 8^\circ$. The reason for that is that it is caused by the bow-shock/separation-shock interaction in the lower flowfield, as mentioned above. However, the upper pressure time signal clearly shows periodic oscillation. That is why the upper u-velocity fluctuation is used for the low-pass filtering of four cases.

In addition, T_{α° becomes smaller with increasing AoA, which indicates that the frequency of flow oscillations increases with the angle of attack, where the

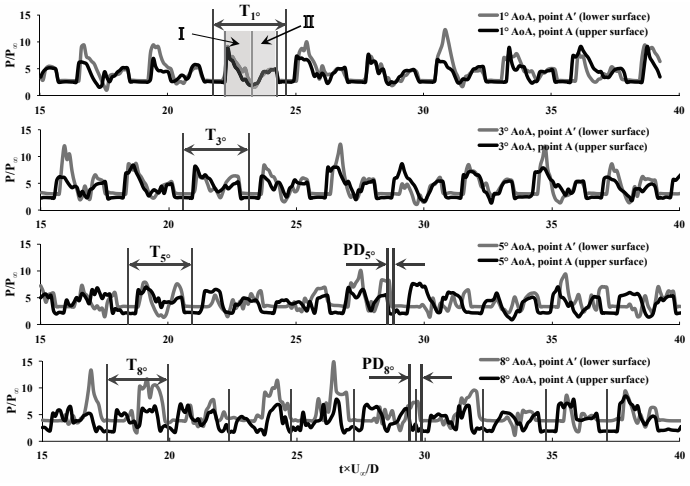

Fig. 7. Pressure time history at point A and A'.

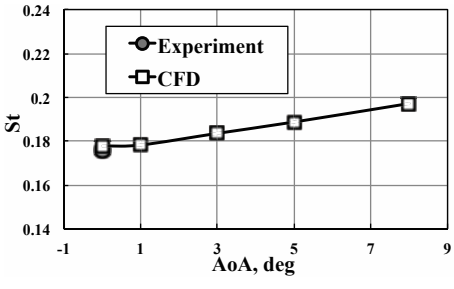

Fig. 8. Strouhal number vs. AoA.

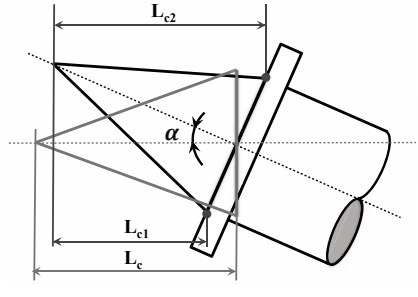

Fig. 9. Schematic of change in attitude with AoA.

frequencies for the cases of $\alpha = 0\,°$,1 °, 3 °, 5 °, and 8 ° are 739 Hz, 741 Hz, 765 Hz, 787 Hz, and 827 Hz, respectively. These values are obtained numerically by using time-averaged data over eight cycles. In the experiment it is 730 Hz in the case with $\alpha = 0\,°$. The corresponding strouhal number [White, 1999], [Williamson, 1988], which is a dimensionless number and used to represent the property of oscillating flow, increases from $St = 0.178$ to 0.197 when AoA changes from 0 ° to 8 °, as expected, where the characteristic length is set to $L = 1.48D \times \cos\alpha$ in this study. The result is shown in Fig. 8.

This change in the reference length of the capsule with AoA is focused and is seen as a major factor for producing the phase difference. A schematic of change in attitude with AoA is shown in Fig. 9, where L_c is the original length of the capsule, and L_{c1} and L_{c2} are the reference lengths for the case with an AoA. When AoA is rather small, L_{c1} becomes smaller than L_c and L_{c2} becomes longer. Therefore, the

characteristic distance of shock wave propagation in the direction of uniform flow can be changed, which leads to different flow oscillations on the upper and lower surfaces of the capsule.

4. Conclusions

A capsule-shaped abort systems using aerodynamic interference was studied by CFD, in which a 3D numerical code was used. The stability of the flowfield before the abort separation was analyzed in detail. The effects of angle of attack were investigated from static simulations at a supersonic speed for the case with no separation distance. The results obtained in this study are summarized as follows:

- The self-sustaining flow oscillations at different AoAs were analyzed and were visualized using the phase averaged data. As AoA increases, the separated flow can be divided into two parts on the capsule surface, which is clearly observed using the numerical results of surface-flow. A large bow shock wave is generated by the upper separated flow, which prevents the lower separated flow from going ahead. As a result, the flow becomes very unstable, especially in the lower flowfield.
- The pressure time signal at two points above the surface in the front of cone was analyzed in detail. The phase difference occurs the value of which becomes larger with increasing AoA. The numerical results show the phase difference 0.04π, 0.12π, 0.28π, and 0.4π when $\alpha = 1\,^\circ$, $3\,^\circ$, $5\,^\circ$, and $8\,^\circ$, respectively. It almost vanishes in the case of $\alpha = 0\,^\circ$. Change in the characteristic lengths of the capsule lead to inconsistent flow oscillations on the upper and lower surfaces of capsule.

Acknowledgments

The experiment described in this research was carried out using the supersonic wind tunnel at the Institute of Space and Astronautical Science (ISAS/JAXA). The authors would like to express their gratitude to ISAS for their support.

References

Cantwell, B. and Coles, D. [1983] "An experimental study of entrainment and transport in the turbulent wake of circular cylinder," *Journal of Fluid Mechanics*, 136, 321.

Chan, W., Klopfer, G., Onufer, J. and Pandya, S. [2008] "Proximity Aerodynamics Analyses for Launch Abort Systems," *AIAA Paper* 2008–7326.

Davidson, J. [2007] "Crew Exploration Vehicle Ascent Abort Overview," *AIAA Paper* 2007–6590.

Hayes, W. P. [2007] "Crew Exploration Vehicle Launch Abort System Flight Test Overview," *AIAA Paper* 2007–6596.

Hussain, A. K. M. F. and Reynolds, W. [1970] "The mechanics of an organized wave in turbulent shear flow," *Journal of Fluid Mechanics*, 41, 241.

Jameson, A. and Baker, T. J. [1983] "Solution of the Euler Equations for Complex Configurations," *AIAA Paper* 83–1929.

Lionel, Larchevêque, Pierre, Sagaut, Ivan, Mary and Odile, Labbé. [2003] "Large-eddy simulation of a compressible flow past a deep cavity." *Physis of Fluids*, **15**(1).

Liou, M S. [1996] "A Sequel to AUSM: AUSM+," *Journal of Computational Physics*, **129**, 364–382.

Mehta, R.C. [2006] "Numerical simulation of supersonic flow past reentry capsules," *Shock Waves*, **15**, 31–41.

Ozawa, H., Kitamura, K., Hanai, K., Miyoshi, M., Mori, K. and Nakamura, Y. [2009] "Abort System Using Supersonic Aerodynamic Interaction for Capsule-Type Space Transportation System," *Journal of the Japan Society for Aeronautical and Space Sciences*, **57**, 175–182 (in Japanese).

Pandya, S., Onufer, J., Chan, W. and Klopfer, G. [2006] "Capsule Abort Recontact Simulation," NASA Technical Report, NASA-06-005; see also *AIAA Paper* 2006–3324.

Pulsonetti, M. V. and Thompson, R. A. [2004] "LAURA Aerodynamic Computations for Space Shuttle Columbia STS-107 Baseline and Damage Scenarios," *AIAA Paper* 2004–2278.

Shima, E. and Jounouchi, T. [1996] "Role of CFD in Aeronautical Engineering (No.14) - AUSM Type Upwind Schemes-," *NAL-SP30, Proceedings of 13th NAL symposium on Aircraft Computational Aerodynamics*, 41–46.

Tamura, Y. and Fujii, K. [1990] "Visualization for Computational Fluid Dynamics and the Comparison with Experiments," *In Proceedings of the AIAA 8th Applied Aerodynamics Conference.*

Van Albada, G. D., Van Leer, B. and Roberts, Jr., W. W. [1982] "A Comparative Study of Computational Methods in Cosmic Gas Dynamics," *Astronomy & Astrophysics (A&A)*, 108, 76–84.

Wang, Y., Ozawa, H., Koyama, H. and Nakamura, Y. [2011] "Simulation of Supersonic Stage Separation of Capsule-Shaped Abort System by Aerodynamic Interaction," *AIAA Paper* 2011–3064.

White, F. M. [1999] *Fluid Mechanics*, 4$^{\text{th}}$ ed., (McGraw Hill), 295–299.

Williams-Hayes, P. [2007] "Crew Exploration Vehicle Launch Abort System Flight Test Overview," *In Proceedings of the AIAA Guidance, Navigation and Control Conference and Exhibit.*

Williamson, CHK. [1988] "Defining a universal and continuous Strouhal-Reynolds number relationship for the laminar vortex shedding of a circular cylinder," *Physics of Fluids*, 31, 2742–2744.